inter.noise 2008 From Silence to Harmony
37th International Congress and Exposition on Noise Control Engineering
26-29 October 2008·Shanghai·China

Vibration of lightweight rib-reinforced structures with random irregularities

Hyuck Chung*, Colin Fox†

* Department of Mathematics, University of Auckland,
Private Bag 92019, Auckland, New Zealand

† Department of Physics, University of Otago,
PO 56, Dunedin, New Zealand

ABSTRACT

This paper describes mathematical modelling procedure of the rib-reinforced floor/ceiling structures, which are made up of components with irregular shapes and physical parameters. Exact determination of the vibration of a composite structure becomes impossible beyond the low-frequency range due to the uncertainties in the structures. Therefore, the prediction model in the mid- to high-frequency range must include the effects of the irregularities. Statistical estimates of the solutions will then give appropriate mean and variance of the vibration of the structure for the given severity of the irregularities. We discuss the nature of the randomness in the lightweight constructions and compare the existing methods, such as Statistical Energy Analysis and Finite Element methods.

1 INTRODUCTION

In this paper, we present a mathematical model of the lightweight timber-based floor/ceiling structures (LTFS), which includes the random uncertainties in the structures' components and construction methods. There has been a strong drive to promote timber-based buildings in recent years. It has also been well known that the timber-based lightweight buildings tend to have poorer sound insulation performances than the concrete counterpart. For that reason, there are many suggestions of innovative designs of LTFS that are made up of many components, such as wooden panels, ribs, joists and glass-fibre wool. As the design becomes complex, conventional deterministic mathematical models can no longer predict the vibration of the structures, particularly in the low- to mid-frequency

*hyuck@math.auckland.ac.nz
†fox@physics.otago.ac.nz

ranges. The focus here is to show how to include the random irregular features of the components in the model.

The modelling method in this paper share the same theoretical foundation with the finite element method (FEM). Both methods derive the stiffness matrix from the Lagrangian of the deformation of the structure. In high frequency ranges, the FEM becomes impractical due to computational cost and the details in the structure, which are often un-measurable. Furthermore, there is no standard procedure in the FEM to include the random irregularities in the structures, such as figure 1. In order to deal with the high-frequency vibration, the statistical energy analysis (SEA) has become a popular method in structural vibration in the past 30 years. The SEA is known to be effective in high-frequency vibration, where there are thousands of modes. However, it is not certain how the method can be applied in the mid-frequency range.

We use the deterministic modelling method to study the effects of random irregularities in individual components and junctions. The SEA, on the other hand, deal with a structures as a collection of elements, between which the energy (due to input excitation) flows. The randomness in the structure is included as the fluctuation in the input and coupling between the elements. There are various hybrid methods that combines the SEA and the FEM, for example by Langley, Shorter and Cotoni [15, 17, 16]. Our and their methods both express the irregularity as the addition to the deterministic stiffness matrix.

$$[D_{\text{det}} + D_{\text{ran}}]\,\mathbf{E} = \mathbf{f}$$

where D_{det} and D_{ran} are the deterministic and the random stiffness matrices, and $\mathbf{E}$ and $\mathbf{f}$ are the energy and the input energy. However, our method is formulated for the deformation of the structure, rather than the energy. Hence, the random part in the components is derived from the Lagrangian of the structure, that is

$$[M_{\text{det}} + M_{\text{ran}}]\,\mathbf{c} = \mathbf{f}$$

where $\mathbf{c}$ is the vector of the coefficients of the Fourier expansion of the deflection of the structure.

A series of papers by Brunskog and Hammer ([1, 2, 3]) show the effects of cavity space and the joists in the LTFS. The papers by Craik ([5, 6]) show the vibration propagation across junctions between flexible plate and beam. Our extensions over their modells are, first: inclusion of coupling between the plate and the joists, and second: inclusion of irregularities of the joist properties. In order to cope with the reallife structures, the model must be able to incorporate the changes without going through the modelling procedure again. For this reason we chose the variational formulation of the system (see Dym and Shames [12]). The solution, in this case the deflection of the components, is the minima of the total energy in the structure. We show how to incorporate the interaction conditions between components, using the typical floor/ceiling configuration shown in figure 1.

The idea of using the power spectral density (PSD) of the irregularities to characterize the randomness can be found in the literature on the scattering in [10], [11] and [14]. In these papers, the fluctuation in the scatterer is characterized by the auto-correlation of the fluctuation, which then describes the scattering cross-section. In Howe [10], the PSD of

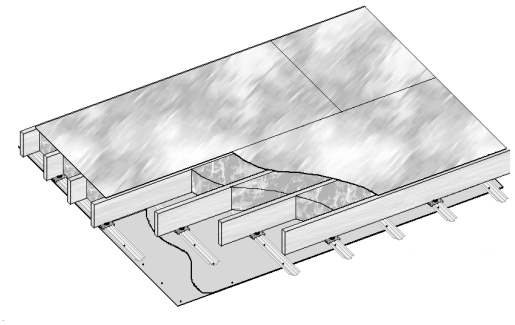

Figure 1: Schematic drawing of an example of the floor/ceiling structure. The upper plate (floor) and the ceiling are joined together by the parallel joists. The cavity space is filled with sound absorbing material and the ceiling is connected by the steel battens running perpendicular to the joists.

the irregularities in an one-dimensional infinite elastic beam is used to estimate the mean energy transfer through the irregular region. We note that, in Howe [10], the solution (deflection of the beam) is decomposed into *coherent* and *incoherent* parts.

$$B\frac{\partial^4 w}{\partial x^4} + m\left(1 + \xi\left(x\right)\right)\frac{\partial^2 w}{\partial t^2} = 0$$

where ξ is the fluctuation in the mass density. The solution is then split into

$$w = \bar{w} + w^1 \tag{1}$$

where $\bar{w}$ and w^1 are the coherent and the incoherent solutions, respectively. The present paper, on the other hand, the solutions are represented using the Fourier basis functions, which have the equally spaced spatial wave modes. We however use the similar method of calculation when the Fourier transform of the irregularities is incorporated using the convolution between the Fourier transform and the infinite-beam modes. It will be shown that the width of the spectra determines the accuracy of the approximation of the solution.

The small perturbation theory is often used to study the irregularities, however it is not appropriate for the class of problem dealing with the interaction between the structure and waves having the similar length scale. As stated in [13], the models using the average values of the parameters do not normally give the average solution in the higher frequency range. In other words, such solution do not represent the reality.

The inclusion of random irregularities in the context of the structural vibration are common in the SEA. However, there are many different definitions of randomness and irregularities depending on the structures. The definitions often seem arbitrary. A series of articles by Langley and others [15, 17, 16] gives detailed description of their definitions of the irregularities in the components and junctions between them. It should be noted that so-called hybrid methods all share the weak-coupling and diffuse-field assumptions

from the SEA. These assumptions are likely invalid for the lightweight structures because of the strong coupling and highly directional energy propagation (see Sjokvist [19]).

The effectiveness of SEA depends on the quality of the parameter called coupling loss factor (CLF), which is the energy loss rate between elements. There are various methods of computing the CLF (see Lyon and DeJong [20]). Shorter and Langley [17, 18] give an SEA application in the structure with the deterministic and the random boundaries. The randomness of the structural properties is assumed to be directly dependent on the randomness of the excitation, which gives the diffuse-field in the SEA sub-systems.

In this paper, the randomness of the components and the junctions is given explicitly using the auto-correlation or the power spectra of the individual irregularities. The deterministic model [4] can include the varying parameters of components and the junction conditions in a similar manner. However, the precise nature of the junction conditions is often unknown or cannot be measured. Therefore, it is substituted with the equivalent energy contribution in the variational formulation of the whole structure.

2 DETERMINISTIC MODEL

We review the deterministic model. The irregularities in the structure are then incorporated using the Fourier representation, which may be geometrical shapes or physical parameters, such as stiffness and mass density. The deflection of the structure is obtained by minimizing the first variation of the Lagrangian of the whole structure. Computation is made easy using the Fourier basis, which expanse the deflection of all individual components. The Fourier representation of the solution enables us to include the irregularities themselves in the structure as their Fourier representation again.

The deformation of an elastic structure is often analyzed using the FEM, which produces the stiffness matrix as the result of minimizing the Lagrangian. The method always comes down to solving the following linear equation.

$$M\mathbf{c} = \mathbf{f}$$

where $\mathbf{c}$ and $\mathbf{f}$ are the deformation and excitation vectors, respectively. The elements of M are derived from the discretizeation of the integrals of the strain and kinetic energies. The size of M is determined by the degrees of freedom, which increase as the frequency becomes large. In contrast to that, M will be derived here using so-called the global elements, which are the Fourier basis functions. Therefore, the elements of $\mathbf{c}$ will be the coefficients of the Fourier expansion instead of the discretised spacial grid points. The following section will show how the irregularities (deviation from the perfect shape or parameter) can be included in M by simple addition of off-diagonal matrices derived from the Fourier transform of the irregularities.

The Lagrangian for the structure is derived on the assumptions of Euler beam and Kirchhof plate, which have only the vertical bending motion (see [8]). These assumptions are justified for the low- to mid-frequency range, in which the shear deformation is small compare to that of the bending motion. The Lagrangian for deflection w, which is a

function of (x, y, t), is given by the following formula.

$$\mathcal{L}(w) = \int_0^T [\mathcal{K}(t) + \mathcal{W}(t) - \mathcal{P}(t)]\, dt \tag{2}$$

where $\mathcal{P}$ and $\mathcal{K}$ are the instantaneous potential and kinetic energies of the structure, respectively. $\mathcal{W}$ is the work done on structure by external forces. The true motion of the structure w makes the Lagrangian stationary, that is,

$$\delta\mathcal{L}(w) = 0,$$

The problem can be simplified by dealing only with time-harmonic vibration at a single frequency ω. The strain energy and the kinetic energy of a Kirchhoff plate ([8]), which is A meter long in the x axis and B meter wide in the y axis, is given by

$$\int_0^A \int_0^B \left\{ \frac{D}{2} \left[\left(\nabla^2 w\right)^2 + 2(1-\nu)\left(w_{xy}^2 - w_{xx}w_{yy}\right) \right] - \frac{1}{2} m\omega^2 w^2 \right\} dxdy, \tag{3}$$

and for an Euler beam we have

$$\frac{1}{2}\int_0^A \left\{ EIw_{xx}^2 - m\omega^2 w^2 \right\} dx \tag{4}$$

where w, D, E, I, ν and m are vertical deflection, flexural rigidity, Young's modulus, moment of inertia (of the beam), Poisson ratio and mass density, respectively.

The mounting conditions (edge conditions) for common floor/ceiling structures are simply supported, which simplifies the expansion on to the sine-functions. The deflection of the upper plate (w_1), ceiling (w_3) and joists (w_2) are,

$$w_i(x, y) = \sum_{m,n=1}^{N} c_{mn}^i \phi_m(x)\, \psi_n(y), \ i = 1, 3, \tag{5}$$

$$w_2(x, j) = \sum_{m=1}^{N} c_{mj}^2 \phi_m(x), \quad j = 1, 2, ..., S_2, \tag{6}$$

where

$$\phi_m(x) = \sqrt{\frac{2}{A}} \sin k_m x, \quad \psi_n(y) = \sqrt{\frac{2}{B}} \sin \kappa_n y \quad m, n = 1, 2, ..., N,$$

and $k_m = \pi m/A$, $\kappa_n = \pi n/B$. The above basis functions satisfy the following orthogonal relationship.

$$\int_0^A \phi_m \phi_n\, dx = \delta_{mn}, \quad \int_0^B \psi_m \psi_n\, dy = \delta_{mn}.$$

The number of joists is denoted by S_2. Note that the summation of the modes is truncated to N to emphasize the computational aspect of the method.

It has been shown in [4, 7] that the air in the cavity space cannot be ignore when considering the low- to mid-frequency vibrations. The acoustic pressure in the cavity is

expressed by the Helmholtz equation. Therefore the acoustic pressure can expanded by the Fourier cosine series in the (x, y) plane because the walls of the cavity is assumed to be acoustically hard. By solving the Helmholtz equation using the separation of variables, acoustic pressure $p(x, y, z)$ can be expanded with coefficients $\Gamma_{mn}^{(1)}$ and $\Gamma_{mn}^{(2)}$.

$$p(x, y, z) = \sum_{m,n=0}^{N} \left(\Gamma_{mn}^{(1)} e^{\gamma_{mn} z} + \Gamma_{mn}^{(2)} e^{-\gamma_{mn} z}\right) \alpha_m(x) \beta_n(y)$$

where $\gamma_{mn} = \sqrt{k_m^2 + \kappa_n^2 - k^2}$ and $k = \omega/c$, c being the speed of sound. The modes are

$$\alpha_m(x) = \sqrt{\frac{2}{A}} \cos k_m x, \quad \beta_n(y) = \sqrt{\frac{2}{B}} \cos \kappa_n y \quad m, n = 0, 1, ..., N.$$

Note that these basis functions satisfy the orthogonal relationship. Acoustic pressure p is then coupled to the plate by the following.

$$\left.\frac{\partial p}{\partial z}\right|_{z=0} = \rho\omega^2 w_1(x, y), \quad \left.\frac{\partial p}{\partial z}\right|_{z=h} = \rho\omega^2 w_3(x, y), \tag{7}$$

where h is the cavity depth. Details of the method of solutions are given in [4, 7].

The energy contribution from the junctions, modelled as elastic connectors, can be included in the Lagrangian as parts of $\mathcal{P}$ in equation 2. The studies by the current authors [4, 7] show that coupling rigidity due to slippage between the upper plate and the joists changes the overall stiffness of the structure, thus shift the locations of the resonant frequencies.

Substituting the Fourier expansions into equations 3 and 4 and using the orthogonal relationship of the basis functions gives the equations of the Fourier coefficients. The strain energy of the plates and the beams can then be expressed using the vectors of the coefficients of the expansion given by

$$\pi_i = \frac{1}{2} \mathbf{c}_i^{\mathrm{t}} M_i \mathbf{c}_i, \quad i = 1, 2, 3,$$

where the index $i = 1, 2, 3$ indicates the upper plate, the joists and the ceiling, respectively. Note that the matrices M_i are diagonal.

$$M_i = D_i \left(k^2 + \kappa^2\right)^2 - m_i \omega^2, \quad i = 1, 3$$
$$M_2 = EIk^4 - m_2 \omega^2,$$

where k and κ are diagonal matrices of $\{k_m\}$ and $\{\kappa_n\}$, respectively.

The joist beams that are in contact with the upper plate, which leads to the following relationship between $\mathbf{c}_1$ and $\mathbf{c}_2$.

$$\mathbf{c}_2 = L\mathbf{c}_1 \tag{8}$$

where matrix L represents the following summation

$$\sum_{n=1}^{N} c_{mn}^1 \psi_n(y_j), j = 1, 2, ..., S_2.$$

The coupling between the components can be included as additional energy contribution. For example, the ceiling is attached to the joists by rubber clips that are designed to isolate the vibration of the joists. Hence, the potential energy of the rubber connectors is

$$\frac{\tau}{2}\sum_{i,j}\left\{w_2\left(x_i,j\right)-w_3\left(x_i,y_j\right)\right\}^2$$

where τ is the spring constant of the rubber connector located at (x_i, y_j). Substituting the Fourier expansion into the above term gives the coupling energy in terms of the Fourier coefficients.

The assembled matrix for the whole system is

$$\mathcal{L}=\frac{1}{2}\mathbf{c}^{\mathrm{T}}\left[\begin{array}{ccc} M_1 & J_{12} & J_{13} \\ J_{21} & M_2 & J_{23} \\ J_{31} & J_{32} & M_3 \end{array}\right]\mathbf{c}+\mathbf{f}^{\mathrm{T}}\mathbf{c}. \tag{9}$$

The off-diagonal sub-matrices J's represent the coupling between the plates and the joists.

Equation 7 give the following relationship between $\mathbf{c}_1, \mathbf{c}_3$ and $\mathbf{\Gamma}$ (vector of $\left\{\Gamma_{mn}^{(1)}\right\}$ and $\left\{\Gamma_{mn}^{(2)}\right\}$)

$$Q_{\mathrm{a}}\mathbf{\Gamma}=\rho\omega^2\left(\begin{array}{c}\mathbf{c}_1\\ \mathbf{c}_3\end{array}\right)$$

where the matrix Q_{a} is derived from the integrals of the products of the basis functions,

$$\int_0^A\int_0^B \phi_m\left(x\right)\psi_n\left(y\right)\alpha_{m'}\left(x\right)\beta_{n'}\left(y\right)\ dxdy.$$

Therefore, the contribution from the air pressure is added in the following form.

$$M_{\mathrm{p}}\mathbf{c}=Q_{\mathrm{a}}\mathbf{\Gamma}+\mathbf{f}.$$

The excitation force vector is given by

$$f_0\phi_m\left(x_0\right)\psi_n\left(y_0\right),\quad m,n=1,2,...,N$$

where (x_0, y_0) is the location of the excitation.

The vectors $\mathbf{c}_0$ and $\mathbf{c}_2$ can be computed from

$$\left[\begin{array}{cc} M_{\mathrm{p}} & -Q_{\mathrm{p}} \\ \rho\omega^2\mathcal{I} & -Q_{\mathrm{a}}\end{array}\right]\left(\begin{array}{c}\mathbf{c}\\ \mathbf{\Gamma}\end{array}\right)=\left(\begin{array}{c}\mathbf{f}\\ 0\end{array}\right). \tag{10}$$

where $\mathcal{I}$ is and identity matrix.

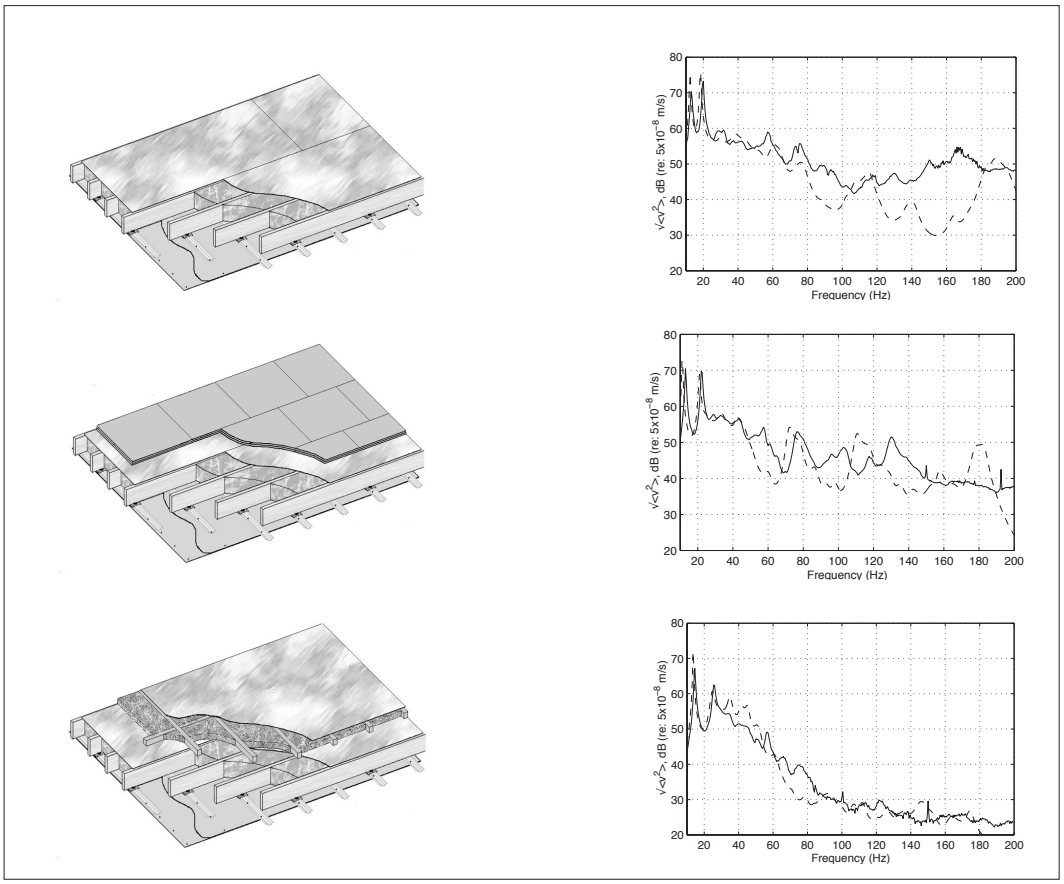

Figure 2: Comparison between the computed and measure surface root average velocity of the ceiling surface. The designs are slightly varied from the top to bottom by having additional layers on the upper surface.

3 RESULTS FROM DETERMINISTIC MODEL

In [4, 7], it is shown that the deterministic model can predict the vibration at a frequency range lower than 80Hz. An examples of the comparison of the root mean squared velocity between the modelling and the experiment results is shown in figure 2. The dimension of the structure is 7m $\times$ 3.2m. The joists are running in the lengthwise direction.

Various experimental mock-up floor/ceiling structures were tested in [7]. Three examples are shown in figure 2 and the parameter of the structures are given in appendix A. The results have confirmed that the models with the deterministic parameters can successfully cope with various design changes in the low frequency range. The variations in the design included, for example, additional layers on the upper plate or joists on the ceiling panels, change of the size of the structure and additional joists on the ceiling panels.

The results of the deterministic modelling shows good agreement with the data up to 80Hz. Above 80Hz, the vibration of the structure is greatly affected by the details in the

components and the design, which are either impossible to be measured or highly irregular from one structure to another. In the following section, we show how the irregular features in the components and the junctions can be included in the model.

4 INCLUSION OF IRREGULARITIES

We consider four examples of the irregularities, which are contact rigidity, joist's Young's modulus (plates and joists) and shape of the joists. These irregularities are defined as the deviation from the ideal constant value. We denote the deviating parameters by

$$\begin{aligned} \theta(x,j), &\text{ joist shape.} \\ \sigma_0+\sigma(x,j), &\text{ contact rigidity,} \\ E+\epsilon(x,j), &\text{ Young's modulus} \\ D+D_{\mathrm{r}}(x,y) &\text{ Young's modulus} \end{aligned}$$

The irregularities, which are represented by the Fourier transform of the irregularity functions, can be included in the solution as the energy contribution. The method of using the Fourier transform or the power spectrum of the irregularities can be found in ([11]) on the scattering of waves by random irregularities. The energy of propagation in a given direction is approximated by the integration of the quadratic form of the covariance of the fluctuation.

Joist shape: The shape of the joist beams is an example of irregularities, which can be measured accurately. The measurement data dry pine beams is shown in figure 3 as the average of the PSD and ten examples of actual measurements. The dimension the beams is approximately 0.1m by 0.2m and the length is 2.4m. The PSD in the figure shows that the beams have mostly two or three twists.

We first take the Taylor expansion of the modes at the contact curves and omit the higher terms because θ is assumed small.

$$\begin{aligned} \psi_n(y_j+\theta(x,j)) &= \sum_{i=0}^{\infty} \frac{(\kappa_n y_j \theta(x,j))^i}{i!} \frac{d^i\psi_n}{dy^i}(y_j) \\ &\approx \psi_n(y_j)+\kappa_n^2 y_j \theta(x,j)\,\beta_n(y_j) \end{aligned} \tag{11}$$

The expansion in equation 11 leads to the following modified contact equation 8.

$$\sum_m c^2_{mj}\phi_m(x) = \sum_{m,n} c^0_{mn}\phi_m(x)\,\psi_n(y_j+\theta(x,j))$$

Using the orthogonal relationship and equation 11 gives

$$c^2_{mj} = \sum_n c^1_{mn}\psi_n(y_j) + \sum_{m',n} q_{nj}c^1_{m'n}\int_0^A \theta(x,j)\,\phi_m(x)\,\phi_{m'}(x)\;dx \tag{12}$$

where $q_{nj}=\kappa_n^2 y_j\beta_n$. Notice that the first term on the right hand side is the same as the one in equation 8. Matrix L_θ represents the second term on the right hand side of equation 12. The irregularity term is now represented by a simple additional matrix.

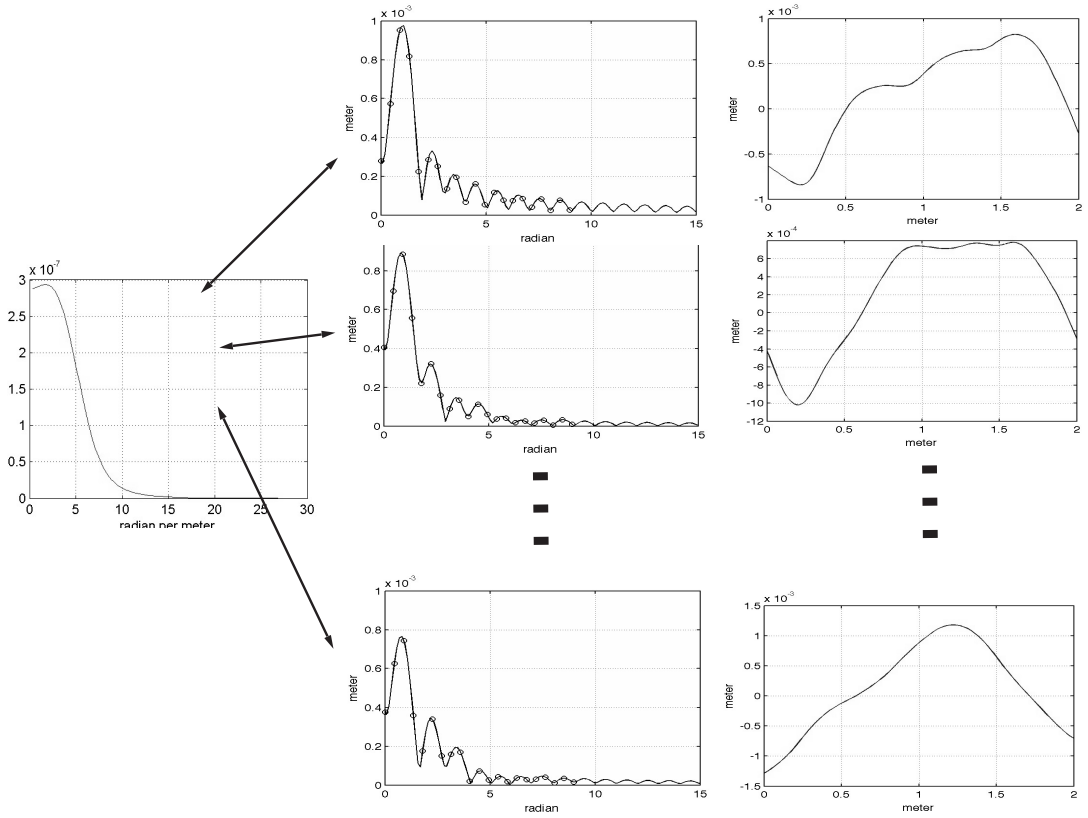

Figure 3: Examples of the Fourier transform of the joist shapes and their samples taken at the mode numbers. The PSD (right) is also given.

The integral in equation 12 can be re-written using the fact that $\{\phi_m\}$ are the Fourier basis functions. The integral is the Fourier transform at the mode numbers $\{k_m, k_{m'}\}$ in a finite interval.

$$\mathbf{c}_2 = [L + L_\theta]\, \mathbf{c}_1.$$

More precisely, the elements of L_θ can be computed by

$$[L_\theta] = q_{nj} \left[\hat{\theta}\left(k_{m-m'}\right) - \hat{\theta}\left(k_{m+m'}\right) \right] \tag{13}$$

We used the following integration relationship to obtain the above.

$$\begin{aligned} &\int_{-\infty}^{\infty} \theta(x) \sin k_m x \sin k_{m'} x \; dx \\ &\qquad = \int_{-\infty}^{\infty} \theta(x) \left\{ e^{\mathrm{i}(k_m - k_{m'})x} - e^{\mathrm{i}(k_m + k_{m'})x} \right\} \; dx \\ &\qquad = \hat{\theta}\left(k_m - k_{m'}\right) - \hat{\theta}\left(k_m + k_{m'}\right). \end{aligned}$$

Note that θ is defined to be zero outside $[0, A]$. The above formula can be rewritten so that the deviation part can appear as additive terms to the regular term. The potential

energy contribution from the beams is then

$$\pi_2 = \frac{1}{2}\mathbf{c}_2^{\mathrm{t}} M_2 \mathbf{c}_2 = \frac{1}{2}\mathbf{c}_1^{\mathrm{t}} \left(L + L_\theta\right)^{\mathrm{t}} M_2 \left(L + L_\theta\right) \mathbf{c}_1.$$

Note that the higher order terms may be used when more details of the shape deviation have to be included.

Stiffness of the joists: The above procedure of sampling the Fourier transform of the irregularity also applies to other examples. The Young's modulus deviation ϵ can be incorporate using the similar procedure as before. The strain energy of the joist beam is

$$\frac{I}{2}\int_0^A \left(E + \epsilon\left(x, j\right)\right)\left\{\frac{d^2 w_2}{dx^2}\left(x, j\right)\right\}^2 \, dx$$

where I is the moment of inertia.

Using the Fourier expansion of w_2 and orthogonality of $\{\phi_m\}$ gives (put the integration formula here)

$$\frac{1}{2}\mathbf{c}_2^{\mathrm{t}}\left\{M_2 + L_\epsilon\right\}\mathbf{c}_2$$

where the elements of L_ϵ are given by

$$\begin{aligned}\left[L_\epsilon\right]_{m,m'} &= I k_m^2 k_{m'}^2 \int_0^A \epsilon\left(x, j\right)\phi_m\left(x\right)\phi_{m'}\left(x\right) \, dx \\ &= I k_m^2 k_{m'}^2 \left[\hat{\epsilon}\left(k_m - k_{m'}\right) - \hat{\epsilon}\left(k_m + k_{m'}\right)\right],\end{aligned}$$

where $\hat{\epsilon}$ is the Fourier transform of ϵ.

Stiffness of the plates: The varying stiffness of the plates can be treated using the 2-dimensional Fourier transform. The integral involving the stiffness of the plate is given by

$$\int_0^A \int_0^B \left\{\frac{D + D_{\mathrm{r}}}{2}\left[\left(\nabla^2 w\right)^2 + 2\left(1 - \nu\right)\left(w_{xy}^2 - w_{xx} w_{yy}\right)\right]\right\} \, dxdy, \tag{14}$$

Using the Fourier expansion of $w\left(x, y\right)$ leads to the similar Fourier representation of $D_{\mathrm{r}}\left(x, y\right)$. Due to the on-homogeneous stiffness, the following integral has to be evaluated.

$$2\left(1 - \nu\right)\int_0^A \int_0^B D_{\mathrm{r}}\left(x, y\right)\alpha_m\left(x\right)\alpha_{m'}\left(x\right)\beta_n\left(y\right)\beta_{n'}\left(y\right) \, dxdy.$$

The above integral can be rewritten as Fourier transform of D_{r} at combinations of the wavenumbers as seen before. Therefore, the irregularity is given by an additional stiffness matrix.

$$\mathbf{c}^{\mathrm{t}}\left[M_1 + M_{\mathrm{ran}}\right]\mathbf{c}. \tag{15}$$

This expression is again similar to the previous representation of the stiffness matrices. The elements of M_{ran} are given by

$$\frac{1 - \nu}{2}\sum \hat{D}_{\mathrm{r}}\left(\pm k_{m \pm m'}, \pm \kappa_{n \pm n'}\right)$$

and

$$\frac{1}{2}\sum \hat{D}_{\mathrm{r}}\left(\pm k_{m\pm m'}, \pm\kappa_{n\pm n'}\right)$$

where $\hat{D}_{\mathrm{r}}$ is the Fourier transform of D_{r} and all combinations of $\pm$ are summed. Notice that the Fourier transform of the irregular part of the stiffness is sampled at the grid points determined by the indices $k_{m\pm m'}$ and $\kappa_{n\pm n'}$.

Contact rigidity: It has been observed in [7, 4] that the overall stiffness of the structure is affected by the contact rigidity at the low- and mid-frequency ranges. Thus the inclusion of contact rigidity shifts the locations of the resonant frequencies of the structure.

We consider the contribution from the slippage as the energy due to deformation of imaginary spring with linear elasticity σ. Thus, the potential energy due to the slippage resistance is

$$\frac{1}{2}\sum_{j=1}^{S_2}\int_0^A \left(\sigma_0 + \sigma\left(x, j\right)\right)\left[\frac{H}{2}\frac{dw_2}{dx}\left(x, j\right)\right]^2 dx$$

where $H = h_0 + h_1$. Notice that the term in $[\cdot]$ is the slippage due to the thickness of the joist and the upper plate.

The resulting energy is also written using the matrices and the vectors of the coefficients.

$$\frac{1}{2}\mathbf{c}_2^{\mathrm{t}}\left[N + L_\sigma\right]\mathbf{c}_2.$$

where the elements of L_σ are derived from the following integrals

$$k_m k_{m'}\left[\hat{\sigma}\left(k_m - k_{m'}\right) + \hat{\sigma}\left(k_m + k_{m'}\right)\right]$$

and the deterministic matrix N is a diagonal matrix of $\sigma_0 H^2 k_m^2/4$.

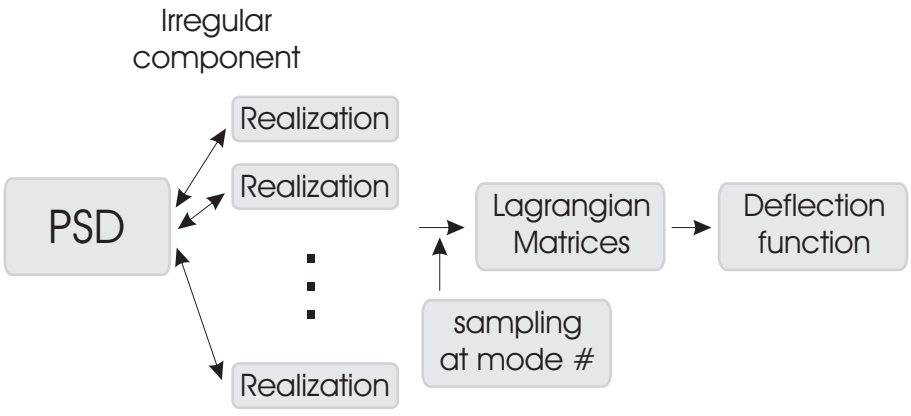

Figure 4: Numerical solutions using the irregular joists. The actual shapes (left column) are converted to the samples of their Fourier transform (middle column), then the resulting root-mean velocity (right column) is shown.

5 SUMMARY

We have shown how the irregularities in the components of the light-weight floor/ceiling structures can be included in the theoretical model. The irregularities are represented by the deviation from the expected values. The deviation is then incorporated into the solution formulae as the Fourier transform sampled at the mode numbers as shown in figure 3. Figure 4 shows the how one can simulate the vibration from the given PSD.

Acknowledgement: H. Chung acknowledges New Zealand Foundation of Research Science and Technology post-doctoral fellowship (Contract number: UOAX0505). Figure 1 is courtesy of G. Schmid of the Acoustics Research Centre.

References

[1] J. Brunskog and P. Hammer, "Models to predict impact sound transmission of lightweight floors, A Literature survey". Journal of Building Acoustic, Volume 7, number 2, (2000).

[2] J. Brunskog and P. Hammer, "Acoustic properties of resilient, statically tensile loaded devices in lightweight structures: A measurement method and statistical analysis," Journal of Building Acoustic, Volume 9, number 2, pp. 99 - 137 (2002).

[3] J. Brunskog and P. Hammer, "Prediction model for the impact sound level of lightweight floors," Acta Acustica united with Acustica, Volume 89, pp. 309-322 (2003).

[4] H. Chung and G. Emms, "Fourier series solutions to the vibration of rectangular light-weight floor/ceiling structures," ACTA Acustica united with Acustica, Vol. 94, pp. 401–409,2008

[5] R.J.M. Craik and R.S. Smith, Sound transmission through lightweight parallel plate. part II: Structure-borne sound, Applied Acoustics, 61, pp.247–269 (2000).

[6] R.J.M. Craik and R.S. Smith, 2000, Sound transmission through double leaf lightweight partitions part I: Air-borne sound, Applied Acoustics, 61, pp.223–245.

[7] G. Emms, H. Chung, G. Dodd, G. Schmid, and K. McGunnigle, "FWPRDC Project PN04.2005 Maximising impact sound resistance of timber framed floor/ceiling systems," The Forest and Wood Products Research and Development Corporation. Australian Government, www.fwprdc.org.au (2006)

[8] F.S. Fahy, "Sound and Structural Vibration," Academic Press Ltd. London, (1985).

[9] M.S. Howe, "Multiple scattering of sound by turbulence and other inhomogeneities," Journal of Sound and Vibration, Volume 27, Number 4, pp. 455-476, 1973.

[10] M.S. Howe, "Multiple scattering of bending waves by random inhomogeneities," Journal of Sound and Vibration, volume 23(3), pp. 279–290, 1972.

[11] I.D. Howells, "The multiple scattering of waves by random irregularities in the medium," Philosophical Transactions of the Royal Society of London. Series A, Mathematical and Physical Sciences, Vol. 252, No. 1015, pp. 431-462, 1960.

[12] I.H. Shames and C.L. Dym, *Energy and finite element methods in structural mechanics*, si units ed., Hemisphere Publishing Corporation, Bristol, (1991).

[13] C.H. Hodges and J. Woodhouse, "Theories of noise and vibration transmission in complex structures," Reports on Progress in Physics, Vol. 49, pp. 107–170, 1986.

[14] G.K. Bachelor,"Small-scale variation of convected quantities like temperature in turbulent fluid: Part 1. General discussion and the case of small conductivity," Journal of Fluid Mechanics, 1959

[15] R.S. Langley and V. Cotoni, "Response variance prediction in the statistical energy analysis of built-up systems," Journal of the Acoustical Society of America, pp. 706–718, Vol 115(2), 2004.

[16] R.S. Langley and V. Cotoni, "Response variance prediction for uncertain vibro-acoustic systems using a hybrid deterministic-statistical method," Journal of the Acoustical Society of America, pp. 3445–3463, Vol 122(6), 2007.

[17] P.J. Shorter and R.S. Langley, "Vibro-acoustic analysis of complex systems," Journal of Sound and Vibration, pp. 669–699, Vol 288, 2005.

[18] P.J. Shorter and R.S. Langley, "On the reciprocity relationship between direct field radiation and diffuse reverberant loading," Journal of the Acoustical Society of America, pp. 85–95, Vol 117(1), 2005.

[19] LG. Sjokvist and J. Brunskog, "Modal analysis for floors in lightweight buildings", Proceedings of InterNoise 2007, Istanbul August, 2007.

[20] R.H. Lyon and R.G. DeJong, "Theory and Application of Statistical Energy Analysis", Butterworth-Heinemann, Boston, 1995.